# Generation of ring dark solitons by phase engineering and their oscillations in spin-1 Bose-Einstein condensates

Shu-Wei Song,[1] Deng-Shan Wang,[2] Hanquan Wang,[3] and W. M. Liu[1]

[1]*Beijing National Laboratory for Condensed Matter Physics, Institute of Physics, Chinese Academy of Sciences, Beijing 100190, China*

[2]*School of Science, Beijing Information Science and Technology University, Beijing 100192, China*

[3]*School of Statistics and Mathematics, Yunnan University of Finance and Economics, Kunming, Yunnan Province 650221, China*

(Received 18 November 2011; revised manuscript received 28 March 2012; published 26 June 2012)

The ring dark solitons in spin-1 $^{23}$Na and $^{87}$Rb Bose-Einstein condensates are studied numerically in the framework of the time-dependent Gross-Pitaevskii equations. By simulating the phase engineering technique in real experiments, we explore the roles of the parameters characterizing the far-off resonant laser pulse which can be used to generate the ring dark solitons. The variations of these parameters have a dramatic effect on the lifetime and the decay profiles of the ring dark solitons. If only one ring dark soliton is generated in one component of the condensate, then ring dark solitons in other components are inclined to be induced, resulting in a coexistence state composed of interdependent ring dark solitons coming from different components of the condensate. Ring dark solitons in this coexistence state exhibit dynamical oscillations for hundreds of milliseconds. By studying the lifetime and decaying profiles of ring dark solitons, we explore the similarities and differences of $^{23}$Na and $^{87}$Rb condensates. In addition, taking into account the fact that the center of the ring may not coincide with that of the trap, we study the dynamics and decaying profiles of the off-centered ring dark solitons in the presence of the symmetry-breaking effect.

DOI: 10.1103/PhysRevA.85.063617 PACS number(s): 03.75.Lm, 03.75.Mn, 05.45.Yv

## I. INTRODUCTION

Since the experimental realization of Bose-Einstein condensates (BECs), intensive interest has been growing and the condensate has been a popularly investigated platform for various effects of quantum many-body interaction. This opens a new field of exploring various types of excitations such as bright solitons, dark solitons, and vortices [1–3]. The concept of a ring dark soliton was introduced theoretically and realized experimentally in nonlinear optics [4–6]. Theocharis *et al*. investigated the ring dark solitons in scalar BEC with a disk-shaped trap [7–11]. Recently, dark-bright stripe solitons and ring dark solitons in two-component BEC are studied and the stable ring dark-bright solitons are found [12,13]. The deep ring dark soliton in scalar BEC has been found to be always unstable towards the formation of vortices. However, it is shown in Ref. [12] that the presence of the "bright" component has a stabilizing effect on the symbiotic state.

As far as we know, ring dark solitons in spin-1 BEC have not been investigated theoretically or experimentally yet. Spinor BECs liberate the spin degrees of freedom of the atoms confined in optical traps. Several phases are possible below the transition temperature $T_c$, and this kind of diversity leads to a fascinating area of research for quantum gases. The magnetic moment accompanying the spin gives rise to magnetism, resulting in excitations such as spin domains, spin textures, and fractional vortices [14,15]. In addition, matter-wave dark solitons can be created experimentally by means of various methods, including the phase engineering and density engineering techniques [16–20]. In particular, Wright *et al*. [21] have achieved spatially varying control of the amplitude and phase of the spinor order parameter. To shed light on the manipulation of ring dark solitons in spinor BEC, we investigate the generations and oscillations of the ring dark solitons in spin-1 BEC by simulating the phase engineering technique.

In the present paper, we explore the dynamical generation and evolution of the ring dark solitons in $F = 1$ $^{23}$Na and $^{87}$Rb condensates. By using models to simulate the phase engineering technique in the experiments, we study the effect of two key parameters of the far-off resonant laser pulse on the dynamics of the ring dark solitons, the width of the laser-induced Stark-shift potential, and the duration of the laser beam. We study the generation and dynamics of the coexistence state of ring dark solitons that is induced by producing only one ring dark soliton in one component of the condensate. Numerical results are compared between $^{23}$Na and $^{87}$Rb condensates.

The rest of the paper is organized as follows. In Sec. II, we introduce the mean-field theoretical model of spin-1 BEC, and a phase distribution model to imitate the phase configuration of the order parameter after the illumination of the laser beam. In Sec. III, we obtain the ground states of the spin-1 $^{23}$Na and $^{87}$Rb condensates numerically, then study the generation process of the ring dark solitons and investigate the roles of parameters characterizing the far-off resonant laser pulse. Section IV focuses on the emergence, oscillation, and decay of the coexistence state of ring dark solitons that is induced by the ring dark soliton in one component of the condensate. Finally, the conclusions are summarized in Sec. V.

## II. THE THEORETICAL MODEL

Most BECs in ultracold atomic gases have internal degrees of freedom originating from the spin. For the $^{87}$Rb and $^{23}$Na atoms, there are spin combinations with $S = 1/2$ (electronic spin) and $I = 3/2$ (nuclear spin), so the total spin $F$ can be chosen to be $F = 1$ or $F = 2$. Both spin-1 and spin-2 atomic condensates are investigated experimentally and theoretically [14,22–31]. For $F = 1$, there are three sublevel states with magnetic quantum number $m = 0, \pm 1$. Within the mean-field

 ©2012 American Physical Society

description, the spin-1 cold-atom condensate can be described by a vectorial order parameter $\Psi = (\psi_1, \psi_0, \psi_{-1})^T$ (the superscript $T$ stands for the transpose), where the component $\psi_m$ $(m = 0, \pm 1)$ denotes the macroscopic wave function of the atoms condensed in the hyperfine state $|F = 1, m\rangle$. The dynamics of the vectorial order parameter follows the multicomponent Gross-Pitaevskii equations (GPEs) [22,33]

$$
\begin{aligned}
i\hbar\frac{\partial\psi_1}{\partial t} &= \left(-\frac{\hbar^2}{2M}\nabla^2 + V\right)\psi_1 + (c_0 + c_2)(|\psi_1|^2 + |\psi_0|^2)\psi_1 \\
&\quad + (c_0 - c_2)|\psi_{-1}|^2\psi_1 + c_2\psi_0^2\psi_{-1}^*, \\
i\hbar\frac{\partial\psi_0}{\partial t} &= \left(-\frac{\hbar^2}{2M}\nabla^2 + V\right)\psi_0 + (c_0 + c_2)(|\psi_1|^2 + |\psi_{-1}|^2)\psi_0 \\
&\quad + c_0|\psi_0|^2\psi_0 + 2c_2\psi_1\psi_0^*\psi_{-1}, \\
i\hbar\frac{\partial\psi_{-1}}{\partial t} &= \left(-\frac{\hbar^2}{2M}\nabla^2 + V\right)\psi_{-1} \\
&\quad + (c_0 + c_2)(|\psi_{-1}|^2 + |\psi_0|^2)\psi_{-1} \\
&\quad + (c_0 - c_2)|\psi_1|^2\psi_{-1} + c_2\psi_0^2\psi_1^*,
\end{aligned}
\tag{1}
$$

where $\nabla^2 = \partial^2/\partial x^2 + \partial^2/\partial y^2 + \partial^2/\partial z^2$, $c_0 = 4\pi\hbar^2(a_0 + 2a_2)/3M$, and $c_2 = 4\pi\hbar^2(a_2 - a_0)/3M$ ($M$ is the atomic mass). $a_0$ and $a_2$ are the $s$-wave scattering lengths corresponding to the total spin of the two colliding bosons 0 and 2, respectively. The ground state of the condensate is ferromagnetic for $c_2 < 0$ and antiferromagnetic for $c_2 > 0$. $V = M(\omega_x^2x^2 + \omega_y^2y^2 + \omega_z^2z^2)/2$ (where $\omega_{x,y,z}$ is the confinement frequency in the corresponding direction) is the external potential. The density of particles is defined by $n = \sum_m |\psi_m|^2$ $(m = 0, \pm 1)$ and the total particles number $N = \int n d\vec{r}$.

To investigate the ring dark solitons in a pancake condensate, we choose $\omega_z \gg \omega_x = \omega_y$, and the three-dimensional (3D) GPEs (1) can be reduced to 2D GPEs. After the dimensionless process (we denote the order parameter with the same $\psi_m$), we have

$$
\begin{aligned}
i\frac{\partial\psi_1}{\partial t} &= \left[-\frac{1}{2}\left(\frac{\partial^2}{\partial x^2} + \frac{\partial^2}{\partial y^2}\right) + \frac{1}{2}\Omega^2(x^2 + y^2)\right]\psi_1 \\
&\quad + [(\alpha_n - \alpha_s)|\psi_{-1}|^2 + (\alpha_n + \alpha_s)(|\psi_0|^2 + |\psi_1|^2)]\psi_1 \\
&\quad + \alpha_s\psi_{-1}^*\psi_0^2, \\
i\frac{\partial\psi_0}{\partial t} &= \left[-\frac{1}{2}\left(\frac{\partial^2}{\partial x^2} + \frac{\partial^2}{\partial y^2}\right) + \frac{1}{2}\Omega^2(x^2 + y^2)\right]\psi_0 \\
&\quad + [(\alpha_n + \alpha_s)(|\psi_1|^2 + |\psi_{-1}|^2) + \alpha_n|\psi_0|^2]\psi_0 \\
&\quad + 2\alpha_s\psi_0^*\psi_{-1}\psi_1, \\
i\frac{\partial\psi_{-1}}{\partial t} &= \left[-\frac{1}{2}\left(\frac{\partial^2}{\partial x^2} + \frac{\partial^2}{\partial y^2}\right) + \frac{1}{2}\Omega^2(x^2 + y^2)\right]\psi_{-1} \\
&\quad + [(\alpha_n + \alpha_s)(|\psi_0|^2 + |\psi_{-1}|^2) \\
&\quad + (\alpha_n - \alpha_s)|\psi_1|^2]\psi_{-1} + \alpha_s\psi_1^*\psi_0^2,
\end{aligned}
\tag{2}
$$

where $\alpha_n = N\sqrt{M^3\omega_z/(2\pi\hbar^5)}c_0$, $\alpha_s = N\sqrt{M^3\omega_z/(2\pi\hbar^5)}c_2$, and $\Omega = \omega_x/\omega_z$. The particle-number conservation condition becomes $\int\sum_m |\psi_m|^2 d\vec{r} = 1$ $(m = 0, \pm 1)$. The time and length are measured in units of $\omega_z^{-1}$ and $\sqrt{\hbar/(M\omega_z)}$, respectively. Based on the 2D GPEs (2), we are going to shed light on the dynamical properties of ring dark solitons in spin-1 BEC.

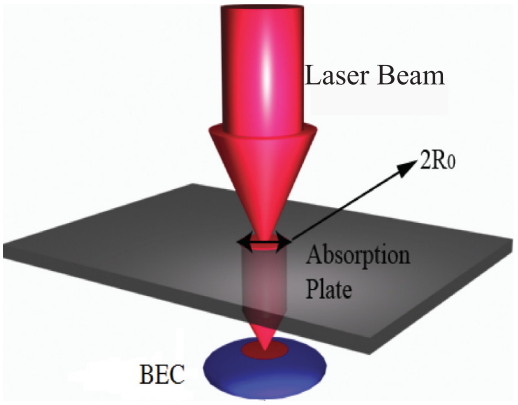


FIG. 1. (Color online) A schematic of imprinting phase steps onto the condensate. The far-off resonant laser pulse (light red) goes through an absorption plate (gray), which is used to modulate the laser. The modulated laser pulse illuminates the cold-atomic condensate (blue) and produces an expected phase configuration. Here, $R_0$ is the radius of the ring dark soliton that is to be created.

Experimentally, the matter-wave dark solitons can be created by means of various methods, such as phase engineering, density engineering, and quantum-state engineering [3,16–19,21,32]. Here we study the dynamics of ring dark solitons by simulating the phase engineering technique [3,16,17,32].

We suppose that $\omega_\perp = \omega_x = \omega_y = (2\pi) \times 12$ Hz and $\omega_z = (2\pi) \times 372$ Hz, respectively. As in Ref. [33], we choose $a_0 = 46a_B$, $a_2 = 52a_B$ ($a_B$ is the Bohr radius) for $^{23}$Na condensate and $a_0 = 110a_B$, $a_2 = 107a_B$ for $^{87}$Rb condensate. And we numerically trace the dynamics of the ring dark solitons in spin-1 $^{23}$Na and $^{87}$Rb condensates.

Generally, the phase engineering technique consists of passing a far-off resonant laser pulse through an absorption plate, which is used to modulate the spatial distribution of the intensity of the laser beam, and creating the corresponding conservative Stark-shift potential that leads to a space-dependent phase shift in the condensate order parameter. Figure 1 shows the schematic for the generation of ring dark solitons by the phase engineering technique. The laser beam that is applied onto the condensate supplies an effective potential, which would produce phase distributions in the condensate order parameter. The laser beam is pulsed on for a time $\delta t$, which is much smaller than the correlation time of the condensate. The phase factor imprinted on the condensate can be adjusted by varying $\delta t$. We use the following model to simulate the phase distribution after illustration of the laser beam:

$$
\phi(x, y) = \frac{\triangle\phi}{2}\left[1 + \tanh\left(\frac{R_0 - \sqrt{x^2 + y^2}}{\Delta x}\right)\right], \tag{3}
$$

where $\Delta\phi$ and $R_0$ are the total phase difference and the radius of the ring dark soliton, respectively. $\Delta x$ reveals the width of the potential edge (induced by the laser beam).

## III. STRUCTURES OF RING DARK SOLITONS

The ground state is antiferromagnetic for the $^{23}$Na condensate and ferromagnetic for the $^{87}$Rb condensate. Because

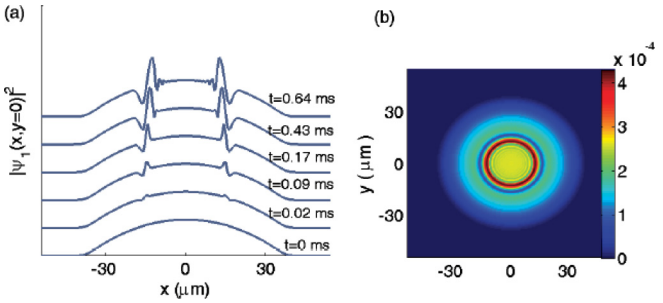


FIG. 2. (Color online) (a) The one-dimensional (1D) density distribution $|\psi_1(x,y=0)|^2$ showing the emergence of a ring dark soliton in the $\psi_1$ component of the $^{23}$Na condensate with a total number of atoms $N_{\rm Na}=10^5$, $\Delta x=0.54$ $\mu$m, $\Delta\phi=\pi$, and $R_0=15.77$ $\mu$m. (b) The ring dark soliton configuration in the $\psi_1$ component of the $^{23}$Na condensate at $t=0.64$ ms. For the $^{87}$Rb condensate, the process of generating and configuration of the ring dark soliton show no significant difference compared to the $^{23}$Na condensate.

all spinors related to each other by gauge transformation $e^{i\theta}$ and spin rotations $U(\alpha,\beta,\gamma)$ ($\alpha,\beta,\gamma$ are Euler angles) are degenerate [33], the ground vectorial order parameter $(\Phi_1,\Phi_0,\Phi_{-1})$ [34] in our numerical results is only one of them. The ground state of the $^{23}$Na condensate does not have the component with magnetic quantum number $m=0$. In certain cases, we use the ground state of the $^{23}$Na condensate that is produced by rotating the numerically obtained ground state in the spin-1 space. We choose the rotating operation as $U(0,\pi/2,\pi/4)$ to produce number balanced states in $\Phi_1$ and $\Phi_{-1}$ components.

After the illustration of the far-off resonant laser pulse, the matter-wave function can be written as

$$\Psi=(\psi_1,\psi_0,\psi_{-1})^T=(\Phi_1,\Phi_0,\Phi_{-1})^T e^{i\phi(x,y)}, \qquad (4)$$

where $\phi(x,y)$ is the phase distribution after the illumination of the laser beam, as modeled in Eq. (3).

As a far-off resonant laser pulse passes through the condensate, all three components of the condensate feel the same conservative Stark-shift potential, and ring dark solitons in different components come up with the same configuration. Therefore, we just show one component to exhibit the early stages of the dynamics of the condensate. Using initial conditions $\Psi$ in Eq. (4) with the numerical ground state before the rotation in the spin space, we show the generation process of the ring dark solitons in the $\psi_1$ component of $^{23}$Na condensate in Fig. 2 with a total number of atoms $N_{\rm Na}=10^5$, $\Delta\phi=\pi$, $\Delta x=0.54$ $\mu$m, and $R_0=15.77$ $\mu$m. As the total phase difference is imprinted onto the condensate, the density in each component begins to redistribute, and one obvious ring dark soliton appears, as shown in Fig. 2(a). At about $t=0.02$ ms, the ring dark soliton begins to appear, and a bright one is forming up simultaneously inside the dark ring. Actually, the relative position of the dark and bright ring is related to the phase gradient properties, as found in Ref. [3].

There are two key parameters in the phase engineering technique, i.e., $\Delta x$, which reveals the width of the potential edge, and the phase difference $\Delta\phi$. As the numerical results in Fig. 3 show, the phase difference at $t=0.21$ ms is smaller than the corresponding initial value. In fact, the phase gradient

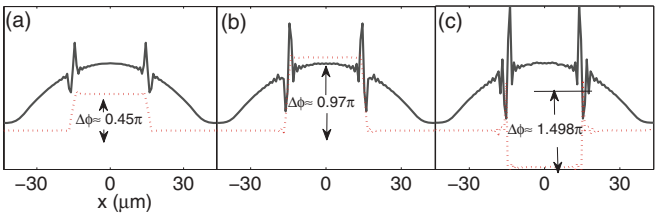


FIG. 3. (Color online) The 1D density $|\psi_1(x,y=0)|^2$ (solid line) and phase distribution $\phi(x,y=0)$ (dotted line) at $t=0.21$ ms in the $^{87}$Rb condensate with $N_{\rm Rb}=2.5\times10^4$, $\Delta x=0.54$ $\mu$m, $R_0=15.77$ $\mu$m, and (a) $\Delta\phi=\pi/2$, (b) $\Delta\phi=\pi$, (c) $\Delta\phi=3\pi/2$, respectively.

increases the total energy of the system, and the depleted phase differences are compensated in the form of the fringes of the density distribution, as we can see from Figs. 3(b) and 3(c). When $\Delta\phi=3\pi/2$, a second, much-shallower ring dark soliton appears, as shown in Fig. 3(c). For Figs. 3(a) and 3(b), the particle density in the trough chooses a finite value (meaning not a black one), whereas the generated ring dark soliton takes a nearly black form with respect to the density characteristics in Fig. 3(c). When we further increase the total phase difference, such as $\Delta\phi=2\pi$, $3\pi$, more ring dark solitons will come up and show collective oscillations.

Next, we aim to find out the effects of the Stark-shift potential edge width on the dynamics of the ring dark solitons through varying $\Delta x$. As $\Delta x$ varies from 2.17 to 0.25 $\mu$m, the generated ring soliton gets darker and darker. But when $\Delta x<0.54$ $\mu$m, the lifetime of the ring dark soliton decreases fiercely and the ring dark soliton shows different decay configurations. Using the initial condition modeled in Eq. (4) for the $^{87}$Rb condensate, Fig. 4 shows the phase of the $\psi_1$ component in the $x$ direction with the dashed (solid) line corresponding to $\Delta x=1.09$ $\mu$m (0.25 $\mu$m). We can see that the phase jump is nearly the same, except for small amplitude oscillations for the $\Delta x=0.25$ $\mu$m case. These two cases correspond to different decay properties of ring dark solitons. For $\Delta x=0.25$ $\mu$m, the lifetime of the ring dark solitons is shorter, and eight vortex and antivortex pairs are produced. But for $\Delta x=1.09$ $\mu$m, the ring

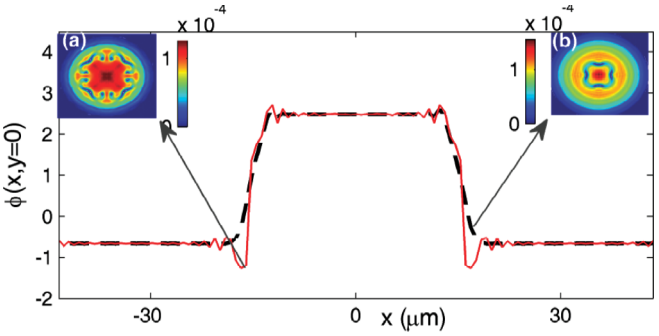


FIG. 4. (Color online) The 1D phase distribution $\phi(x,y=0)$ at $t=0.43$ ms in the $\psi_1$ component of the $^{87}$Rb condensate with parameters $R_0=15.77$ $\mu$m, $\Delta\phi=\pi$, $\Delta x=1.09$ $\mu$m (dashed line), and $\Delta x=0.25$ $\mu$m (solid line). (a) and (b) show the corresponding different density decay profiles of the ring dark solitons at $t=12.84$ ms and $t=57.76$ ms, respectively.

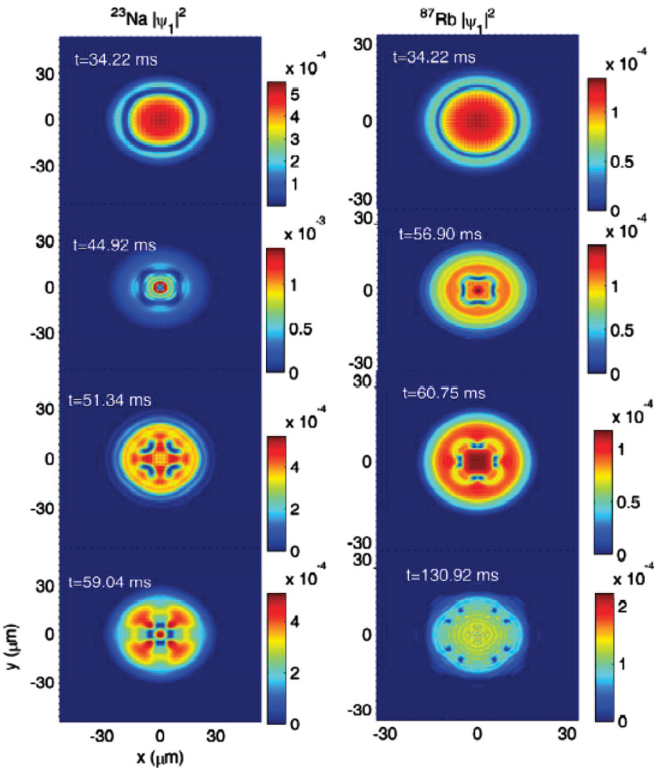


FIG. 5. (Color online) The density distribution $|\psi_1|^2$ of the decaying ring dark solitons in the $^{23}$Na and $^{87}$Rb condensates with parameters $N_{\rm Na} = N_{\rm Rb} = 2.5 \times 10^4$, $R_0 = 8.16\,\mu$m, $\Delta\phi = 1.05\pi$, and $\Delta x = 0.56\,\mu$m. Other components of the condensate exhibit the same dynamic configuration. The initial condition is modeled by Eq. (4) with the numerical ground state before rotation in the spin space.

dark soliton can last as long as 57.76 ms, and finally decays into four vortex and antivortex pairs. This can be understood by resorting to the healing length $\xi = 1/\sqrt{8\pi an}$ [35]. The size of topological excitations such as dark solitons and vortices is fixed by the healing length [35]. And for the $^{87}$Rb condensate in our system, $\xi \approx 0.55\ \mu$m, so it is reasonable to assume the instability of the soliton structures with $\Delta x < 0.55$ ms. In Fig. 4, the notable oscillation of the phase distributions around the slope enhances the decay of the ring structures.

To explore the differences of the dynamics of the ring dark solitons between the $^{23}$Na and $^{87}$Rb condensates, we plot the density distributions of the decaying ring dark solitons. As shown in Fig. 5, the density distribution of the $\psi_1$ component of the $^{23}$Na and $^{87}$Rb condensates exhibits the different decaying dynamics. At $t = 34.22$ ms, nearly black ring dark solitons have formed in both condensates. However, ring dark solitons in the $^{23}$Na, which break into $x$-like vortex pairs, live a shorter lifetime compared to that in the $^{87}$Rb condensate, which break into $+$-like vortex pairs. The dynamics of the vortex pairs is the same as found by Ref. [7] in scalar BEC. The configuration of the vortex and antivortex pairs oscillates between the $x$- and $+$-like configurations, while the ring periodically shrinks and expands.

If all of the components of the condensate bear the same parameterized ring dark solitons, then the total density distribution of the condensate exhibits the same profile as that in each component. When detected in the experiment with the time-of-flight technique, the profiles of ring dark solitons do not show differences from that in scalar BEC. In Table I, we summarize the lifetimes of ring dark solitons in different systems of BEC, according to Refs. [7,10] and our numerical calculations. We note that with certain parameters (as shown in Fig. 5) in the $^{87}$Rb condensate, the lifetime of the nearly black ring soliton in spinor BEC without Feshbach resonance management (FRM) is remarkably prolonged compared to the lifetime of the ring dark soliton in scalar BEC. And this lifetime scale is comparable with the lifetime of a shallower ring dark soliton (the total phase difference is $\Delta\phi = 0.707\pi$) in Ref. [10]. It would be useful to explore ways to prolong the lifetime of the ring dark solitons by varying the parameters of the external potentials or the spin-dependent and -independent interactions.

TABLE I. Lifetime of the ring dark solitons in different BEC systems. For the scalar BEC with Feshbach resonance management (FRM), the total phase difference is $\Delta\phi = 0.707\pi$, which should be a key factor for long-lived ring dark solitons. For the spinor $^{23}$Na or $^{87}$Rb BEC case, ring dark solitons with total phase difference $\Delta\phi \approx \pi$ are generated in each component of the condensate.

| Systems of BEC | Lifetime ($1/\omega_\perp$) |
|---|---|
| Scalar BEC without FRM | 1.14 |
| Scalar BEC with FRM | 5.09 |
| Spinor $^{23}$Na BEC without FRM | 3.48 |
| Spinor $^{87}$Rb BEC without FRM | 4.30 |

## IV. INDUCED AND OFF-CENTERED RING DARK SOLITONS

### A. Common characteristics of the coexistence state of ring dark solitons in $^{23}$Na and $^{87}$Rb condensates

In real experiments, the far-off resonant laser pulse is not ideal, so we consider symmetry-breaking effects in our simulation by allowing the trap center to randomly jump within a region $[-\delta,\delta] \times [-\delta,\delta]$ ($\delta = 0.002h$, where $h$ is the grid size).

We suppose that the condensate takes phase patterns as

$$\Psi = (\psi_1, \psi_0, \psi_{-1})^T = (\Phi_1 e^{i\phi(x,y)}, \Phi_0, \Phi_{-1})^T. \qquad (5)$$

On this occasion, the ring dark soliton is formed in the first component, and at the same time, ring dark solitons in other components are induced. In addition, the mutual filling of different components supplies effective potentials to support the ring dark soliton structure in each component, resulting in a coexistence structure which can live hundreds of milliseconds.

In Fig. 6, we plot the 1D density and phase distributions of the three components at $t = 0.43$ ms for the $^{87}$Rb condensate. We find that the ring dark soliton in the $\psi_1$ component has been formed, while another two much-shallower dark solitons in the $\psi_0$ and $\psi_{-1}$ components germinate, as slight phase jumps are in their way (see the bottom panel). In fact, the atoms in the $\psi_0$ and $\psi_{-1}$ components fill the density gap in the $\psi_1$ component, resulting in a complex interdependent structure. After the full generation of ring dark solitons in all three components, the coexistence structure oscillates complicatedly.

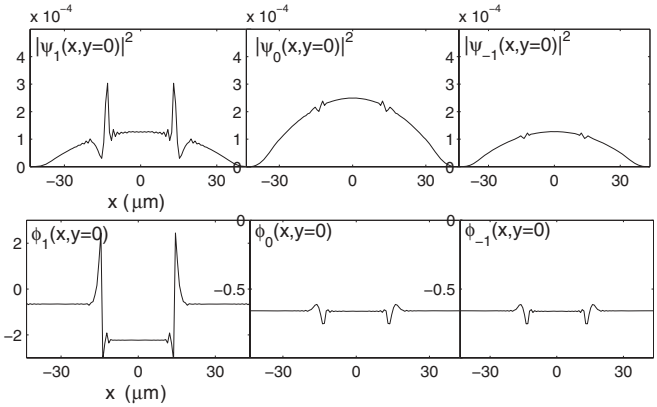


FIG. 6. The 1D density (top panels) and phase (bottom panels) distribution at $t = 0.43$ ms for the three components of the $^{87}$Rb condensate, with $N_{\rm Rb} = 2.5 \times 10^4$, $R_0 = 15.77$ $\mu$m, $\Delta\phi = 3\pi/2$, and $\Delta x = 1.09$ $\mu$m.

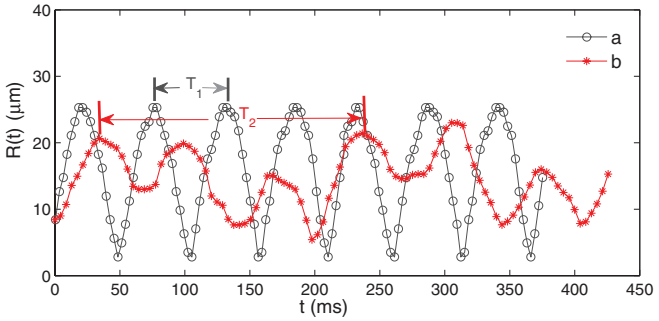


FIG. 8. (Color online) The time evolution of the radius of the ring dark solitons in $^{23}$Na condensate with $N_{\rm Na} = 2.5 \times 10^4$, $R_0 = 8.16$ $\mu$m, and $\Delta x = 0.56$ $\mu$m. Line $a$: radius of ring dark solitons produced by generating the same parameterized ring dark solitons in each component of the condensate with an initial total phase difference $\Delta\phi = 0.5\pi$; line $b$: radius of ring dark solitons produced by generating one ring dark soliton in one component of the condensate with an initial total phase difference $\Delta\phi = 1.05\pi$.

In order to exhibit some aspects of the complex oscillating properties, we depict the darkness of the solitons in different components (the velocity of the dark soliton is connected to the darkness) [36]. In our numerical calculation, both the $^{23}$Na and $^{87}$Rb condensates exhibit a darkness-transferring property between different components. Figure 7 shows the dynamical process of the transferring for the $^{23}$Na condensate using an initial condition modeled by Eq. (5) with a ground state directly obtained by imaginary-time evolution. At $t = 67.60$ ms, the nearly black ring soliton appears in the $\psi_{-1}$ component. And by $t = 121.50$ ms, the darkness of the ring soliton in the $\psi_{-1}$ component has totally been transferred onto the $\psi_1$ component [as shown in Fig. 7(b)]. After 37.65 ms, the ring dark soliton restores its darkness in the $\psi_1$ component, as shown in Fig. 7(c). For the phase distribution model in Eq. (5) and parameters in Fig. 7, the coexistence structure in both the $^{23}$Na and $^{87}$Rb condensates can live more than 800 ms.

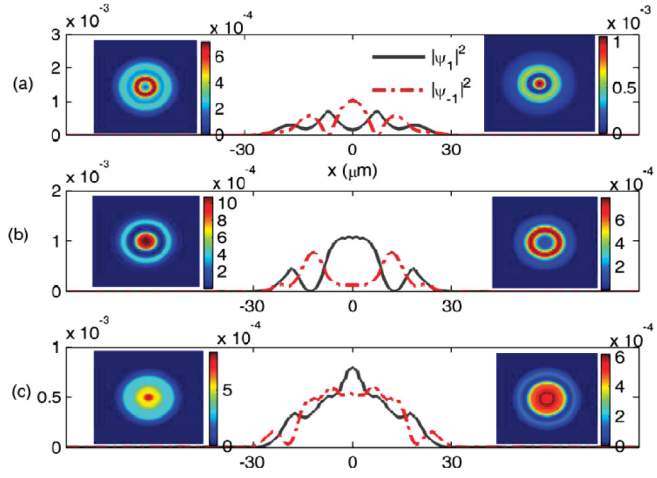


FIG. 7. (Color online) The 1D density distribution at $t =$ (a) 67.60 (b) 121.50, and (c) 159.15 ms in $\psi_1$ (solid line) and $\psi_{-1}$ (dash-dotted line) components of the $^{23}$Na condensate showing the "darkness-transferring" effect with $N_{\rm Na} = 2.5 \times 10^4$, $R_0 = 8.16$ $\mu$m, $\Delta\phi = 1.05\pi$, and $\Delta x = 0.56$ $\mu$m. The 2D density distributions according to each time point are attached for $\psi_1$ (left) and $\psi_{-1}$ (right). The density of the $\psi_0$ component (which is of the order of $10^{-8}$) is omitted.

Even though complicated, the oscillations exhibit periodicity roughly for an initial condition with the absence of the $m = 0$ component. In addition, the oscillation frequency is approximately $0.58\Omega/\sqrt{2}$, which is different from that in the scalar BEC [7,37]. The periodical signature can be seen from Fig. 8, showing the evolutionary radius of the ring dark soliton. In Fig. 8, line $a$ corresponds to the state of generating the same ring dark solitons in all three components of the condensate, while line $b$ corresponds to the state of generating only one obvious ring dark soliton in one component of the condensate. For line $a$, the oscillation frequency is $\omega_o \approx 2.14\Omega/\sqrt{2}$ (roughly consistent with that in Ref. [7] for the scalar BEC), while it is $\omega_o \approx 0.58\Omega/\sqrt{2}$ for line $b$, indicating a prolonged oscillation period. In contrast with the 1D condensate, the ring dark soliton oscillates between the maximum and minimum radius with nearly a two-times-bigger frequency in the 2D condensate. For the coexistence state composed of interdependent ring dark solitons coming from different components of the condensate, the oscillation exhibits periodic character in a rough way because of the interaction and radiation of the ring dark solitons. During the rough oscillation process, a prolonged oscillation period is found. In fact, the oscillation of the ring dark solitons is hindered by the embedded particles of another component, resulting in a low oscillation frequency of the ring dark solitons. We should mention that if we use the initial condition with the appearance of all three components of the condensate, then the oscillation is more complicated and so is the periodicity.

If the coexistence state is induced by an obviously off-centered ring dark soliton, then it suffers an earlier collapse for both the $^{23}$Na and $^{87}$Rb condensates with a time scale of about 150 ms. In the following, taking into account the fact that the center of the ring may not coincide with that of the trap, we suppose an off-centered ring dark soliton with a deviation $\delta p$. The oscillation of the ring dark solitons is sensitive to such a deviation. When the deviation increases to

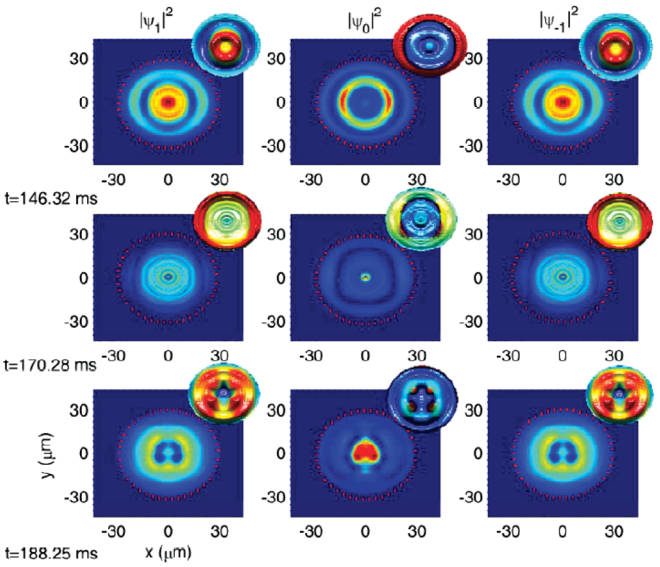


FIG. 9. (Color online) The decaying process shown by the density and phase distributions of the $^{23}$Na condensate with an initial off-centered ring dark soliton in the $\psi_0$ component. The deviation in $y$-direction $\delta p$ is 0.6 $\mu$m and $R_0 = 8.16$ $\mu$m, $\Delta\phi = 3\pi/2$, $\Delta x = 0.56$ $\mu$m. At $t = 146.32$ ms, imbalance in the ring dark solitons appears, and 24.96 ms later, the ring dark soliton distorts in the $\psi_0$ component. The ring dark solitons are totally broken with vortex and antivortex pairs in the $\psi_0$ component at $t = 188.25$ ms.

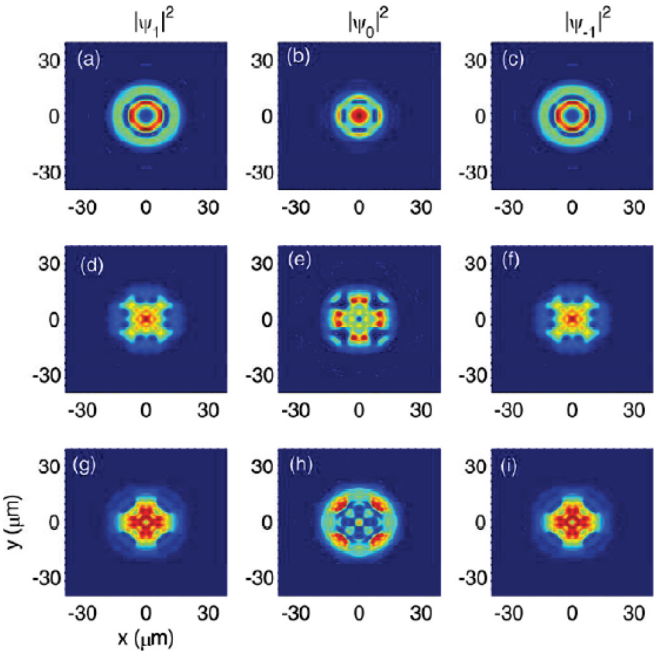


FIG. 10. (Color online) The density distributions $|\psi_1|^2$, $|\psi_0|^2$, and $|\psi_{-1}|^2$ of the $^{87}$Rb condensate at chosen time points with $N_{\rm Rb} = 2.5 \times 10^4$, $R_0 = 8.16$ $\mu$m, $\Delta\phi = 3\pi/2$, and $\Delta x = 0.56$ $\mu$m, showing the decay of the ring dark solitons and motion of the vortex and antivortex pairs. Density configurations are shown at (a)–(c) $t = 123.22$, (d)–(f) $t = 164.28$, and (g)–(i) $t = 189.10$ ms.

the value $\delta p = 0.20$ ms, the lifetime of the ring dark solitons decreases evidently. In Fig. 9, we show the decaying process of the ring dark solitons with $\delta p = 0.60$ $\mu$m for $^{23}$Na. The parameters are the same as that in Figs. 11(a)–11(c). Without deviation $\delta p$, the coexistence state of ring dark solitons can live as long as 320.88 ms and breaks into four pieces in the $\psi_0$ component at $t = 378.64$ ms without the formulation of vortex and antivortex pairs, as shown in Figs. 11(a)–11(c). With a finite $\delta p$, the coexistence state suffers breakdown at a much earlier time. At $t = 146.32$ ms, the darkness of the rings lose their balance, and the darker part of the ring is more inclined to decay into vortices. At $t = 170.28$ ms, the ring structure in the $\psi_0$ component distorts slightly into a form of trapezoid and four vortex and antivortex pairs come up, as shown by the corresponding top-right phase profile panels of Fig. 9. And at $t = 285.50$ ms, the ring dark solitons break down totally. The numerical results show that the lifetime and dynamics of the ring dark solitons are sensitive to such a deviation, indicating that it is very essential in the real experiment to control the relative position of the optical potential and the far-off resonant laser beam which is used to generate the ring dark solitons.

### B. Different aspects of the coexistence state of ring dark solitons in $^{23}$Na and $^{87}$Rb condensates

To explore the differences between $^{23}$Na and $^{87}$Rb condensates in a short time scale, we suppose the initial vector parameter to be

$$\Psi = (\psi_1, \psi_0, \psi_{-1})^T = (\Phi_1, \Phi_0 e^{i\phi(x,y)}, \Phi_{-1})^T, \qquad (6)$$

with the parameters $N_{\rm Na} = N_{\rm Rb} = 2.5 \times 10^4$, $R_0 = 8.16$ $\mu$m, $\Delta\phi = 3\pi/2$, and $\Delta x = 0.56$ $\mu$m. Here, for the $^{23}$Na condensate, the ground state is obtained by the acting of $U(0,\pi/2,\pi/4)$ on the ground state that we obtain from direct numerical calculation.

In this case, the coexistence state structure decays into vortex and antivortex pairs at an earlier time for the $^{87}$Rb condensate. As shown in Fig. 10, at about $t = 123.22$ ms, four vortex and antivortex pairs arranging themselves in a "+" configuration have been formed in the $\psi_0$ component of the condensate while vortex pairs are emerging in the other two components. The vortex and antivortex pairs afterwards arrange themselves in +-like and $x$-like configurations alternatively. Following the vortex configuration in the $\psi_0$ component, the vortex and antivortex pairs take the configuration of + in $\psi_1$ and $\psi_{-1}$ components at $t = 164.28$ ms, while they take the configuration of $x$ in the $\psi_0$ component. At $t = 189.10$ ms, the vortex and antivortex pairs in the $\psi_1$ and $\psi_{-1}$ components catch up with that in the $\psi_0$ component, and evolve into $x$-like configurations. However, this kind of vortex pairs oscillation does not occur in the $^{23}$Na condensate with a time span of 378.64 ms, at which the ring dark solitons break into four pieces in the $\psi_0$ component as shown in Figs. 11(a)–11(c). The insets to the top-right of the density distributions show the phase distributions, showing the absence of the vortex and antivortex pairs. The coexistence state, composed of ring dark solitons coming from different components in the $^{23}$Na condensate, enjoy a longer lifetime than that in the $^{87}$Rb condensate. We ascribe this phenomena to the effect of the spin-dependent interaction parameter $c_2$, which is positive for $^{23}$Na and negative for $^{87}$Rb.

Taking the same parameters in the $^{87}$Rb condensate but with a positive $\alpha_s$ ($\alpha_s = 0.038\alpha_n$ is chosen in our numerical

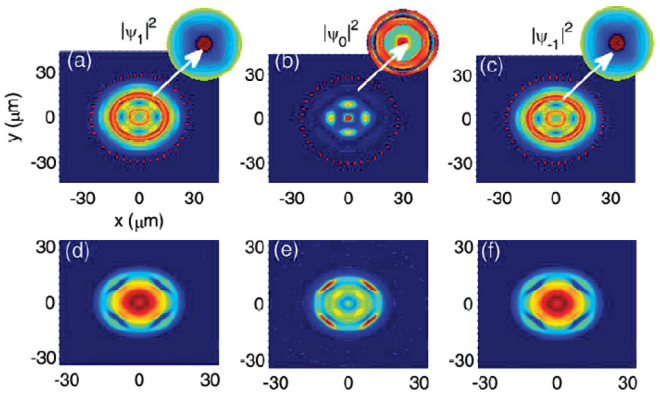


FIG. 11. (Color online) (a)–(c) are the density distributions $|\psi_1|^2$, $|\psi_0|^2$, and $|\psi_{-1}|^2$ of the $^{23}$Na condensate at $t = 378.64$ with $N_{\rm Na} = 2.5 \times 10^4$, $R_0 = 8.16$ $\mu$m, $\Delta\phi = 3\pi/2$, and $\Delta x = 0.56$ $\mu$m. The insets on the top right show the phase distribution of the condensate. (d)–(f) are density distributions at $t = 160.00$ ms with the same parameters as in Fig. 10, except for $\alpha_s = 0.038\alpha_n$. The ground state used has been rotated by $U(0,\pi/2,\pi/4)$ in the spin space.

calculation), we find that the lifetime of the coexistence state composed of ring dark solitons is prolonged remarkably, as show in Figs. 11(d)–11(f). In the real $^{87}$Rb condensate with parameters in Fig. 10, the coexistence state breaks into vortex and antivortex pairs totally at 123.22 ms [Figs. 10(a)–10(c)]. However, the state can last until $t = 160.86$ ms, as shown in Figs. 11(d)–11(f). Different spin-mixing dynamics, which is determined by the spin-dependent interaction term, is found between the $^{23}$Na and $^{87}$Rb condensates, as shown in Fig. 12, and this should be responsible for the different lifetimes of the ring dark solitons between the $^{23}$Na and $^{87}$Rb condensates.

Therefore, ring dark solitons of the ferromagnetic condensate incline to decay into vortex and antivortex pairs much earlier than that of the antiferromagnetic condensate. As it is known, modulational instability is possible in ferromagnetic spinor condensates [23,31]; and the instability would cause the breakdown of exotic structures such as ring dark solitons. Calculations in the present paper show that such a worry is not necessary. The modulational instability has a close dependence on the phase distribution of the state, as found in

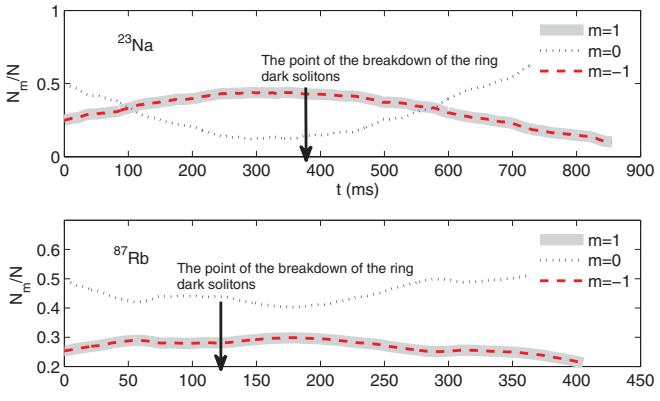


FIG. 12. (Color online) Spin populations vs evolution time of the $^{23}$Na (upper panel) and $^{87}$Rb (bottom panel) condensates with $N_{\rm Na} = N_{\rm Rb} = 2.5 \times 10^4$, $R_0 = 8.16$ $\mu$m, $\Delta\phi = 3/2\pi$, and $\Delta x = 0.56$ $\mu$m. For the $^{23}$Na condensate, a rotated initial ground state is used.

Ref. [31]. By simulating the experimental generation of ring dark solitons, the state in our present setup, which is composed of interdependent ring dark solitons, is not a stationary state. So the condition for the modulational instability in Refs. [23,31] is not well satisfied. We can understand this point by referring to the spin-mixing effect. States that would suffer modulational instability found in Refs. [23,31] do not involve the spin mixing [38] between components of the condensate. In our system, spin mixing occurs at the very beginning, as shown in Fig. 12, which exhibits the spin populations versus evolution time (spin mixing in another parameter region has also been found), indicating the deviation of the state of ring dark solitons from the modulationally instable states obtained in Refs. [23,31].

## V. CONCLUSIONS

In conclusion, the generation and dynamics of the ring dark solitons in both the spin-1 $^{23}$Na and $^{87}$Rb condensates are explored by simulating the phase engineering technique numerically. We find that the characteristics of the far-off resonant laser pulse, such as the Stark-shift potential width (revealed by $\Delta x$) and the duration of the beam $\delta t$ (revealed by $\Delta\phi$), affect the dynamical properties of the condensate dramatically, including the lifetime and the decay profiles of the ring dark solitons. We choose optimal parameters to generate nearly black ring solitons. If only one ring dark soliton in one component of the condensate is generated, then ring dark solitons in other components are induced, and they compose a coexistence state, which exhibits dynamical oscillations for hundreds of milliseconds. The oscillation of the coexistence state can live hundreds of milliseconds because of the mutual filling and spin mixing of different components. The coexistence state is more likely to be stabilized in the presence of all three components of the condensate. The coexistence state can enjoy a longer lifetime in the $^{23}$Na condensate than that in the $^{87}$Rb condensate. However, if the coexistence structure is induced by an obviously off-centered ring dark soliton, then it suffers an earlier collapse with the appearance of vortex and antivortex pairs. This work may help to realize manipulation of ring dark solitons in high-dimensional multicomponent BEC. Because of the long lifetime of the ring structures (more than 800 ms for $^{87}$Rb), we hope that our results can stimulate investigation of high-dimensional ring dark solitons in future spinor BEC experiments. In fact, the density engineering and phase engineering can be utilized together to generate more perfect ring dark structures, whose lifetime should be much longer. In addition, the FR technique is waiting to be used to manipulate ring dark solitons in spinor BEC in the future.

## ACKNOWLEDGMENTS

This work was supported by the NKBRSFC under Grants No. 2011CB921502, No. 2012CB821305, No. 2009CB930701, and No. 2010CB922904, the NSFC under Grants No. 10934010 and No. 60978019, and the NSFC-RGC under Grants No. 11061160490 and No. 1386-N-HKU748/10. D.S.W. was supported by the NSFC under Grant No. 11001263 and by the China Postdoctoral Science Foundation. H.W. was supported by the NSFC under Grant No. 10901134.

[1] M. R. Matthews, B. P. Anderson, P. C. Haljan, D. S. Hall, C. E. Wieman, and E. A. Cornell, Phys. Rev. Lett. **83**, 2498 (1999).

[2] K. E. Strecker, G. B. Partridge, A. G. Truscott, and R. G. Hulet, Nature (London) **417**, 150 (2002).

[3] S. Burger, K. Bongs, S. Dettmer, W. Ertmer, K. Sengstock, A. Sanpera, G. V. Shlyapnikov, and M. Lewenstein, Phys. Rev. Lett. **83**, 5198 (1999).

[4] Y. S. Kivshar and X. Yang, Phys. Rev. E **50**, R40 (1994).

[5] H. E. Nistazakis, D. J. Frantzeskakis, B. A. Malomed, and P. G. Kevrekidis, Phys. Lett. A **285**, 157 (2001).

[6] A. Dreischuh, D. Neshev, G. G. Paulus, F. Grasbon, and H. Walther, Phys. Rev. E **66**, 066611 (2002).

[7] G. Theocharis, D. J. Frantzeskakis, P. G. Kevrekidis, B. A. Malomed, and Y. S. Kivshar, Phys. Rev. Lett. **90**, 120403 (2003).

[8] G. Theocharis, P. Schmelcher, M. K. Oberthaler, P. G. Kevrekidis, and D. J. Frantzeskakis, Phys. Rev. A **72**, 023609 (2005).

[9] S. J. Yang, Q. S. Wu, S. N. Zhang, S. Feng, W. Guo, Y. C. Wen, and Y. Yu, Phys. Rev. A **76**, 063606 (2007).

[10] X. H. Hu, X. F. Zhang, D. Zhao, H. G. Luo, and W. M. Liu, Phys. Rev. A **79**, 023619 (2009).

[11] D. J. Frantzeskakis, J. Phys. A: Math. Theor. **43**, 213001 (2010).

[12] J. Stockhofe, P. G. Kevrekidis, D. J. Frantzeskakis, and P. Schmelcher, J. Phys. B **44**, 191003 (2011).

[13] V. A. Brazhnyi and V. M. Pérez-García, Chaos Soliton Fractals **44**, 381 (2011).

[14] J. Stenger, S. Inouye, D. M. Stamper-Kurn, H. J. Miesner, A. P. Chikkatur, and W. Ketterle, Nature (London) **396**, 345 (1998).

[15] A. E. Leanhardt, Y. Shin, D. Kielpinski, D. E. Pritchard, and W. Ketterle, Phys. Rev. Lett. **90**, 140403 (2003).

[16] Ł. Dobrek, M. Gajda, M. Lewenstein, K. Sengstock, G. Birkl, and W. Ertmer, Phys. Rev. A **60**, R3381 (1999).

[17] J. Denschlag, J. E. Simsarian, D. L. Feder, C. W. Clark, L. A. Collins, J. Cubizolles, L. Deng, E. W. Hagley, K. Helmerson, W. P. Reinhardt, S. L. Rolston, B. I. Schneider, and W. D. Phillips, Science **287**, 97 (2000).

[18] Z. Dutton, M. Budde, C. Slowe, and L. V. Hau, Science **293**, 663 (2001).

[19] N. S. Ginsberg, J. Brand, and L. V. Hau, Phys. Rev. Lett. **94**, 040403 (2005).

[20] I. Shomroni, E. Lahoud, S. Levy, and J. Steinhauer, Nature Phys. **5**, 193 (2009).

[21] K. C. Wright, L. S. Leslie, A. Hansen, and N. P. Bigelow, Phys. Rev. Lett. **102**, 030405 (2009).

[22] T. Ohmi and K. Machida, J. Phys. Soc. Jpn. **67**, 1822 (1998).

[23] H. E. Nistazakis, D. J. Frantzeskakis, P. G. Kevrekidis, B. A. Malomed, and R. Carretero-González, Phys. Rev. A **77**, 033612 (2008)

[24] E. J. Mueller, Phys. Rev. A **69**, 033606 (2004).

[25] W. Z. Bao and Y. Z. Zhang, Methods Appl. Anal. **17**, 049 (2010).

[26] J. Ieda, T. Miyakawa, and M. Wadati, Laser Phys. **16**, 678 (2005).

[27] B. J. Dkabrowska-Wüster, E. A. Ostrovskaya, T. J. Alexander, and Y. S. Kivshar, Phys. Rev. A **75**, 023617 (2007).

[28] P. Szańkowski, M. Trippenbach, E. Infeld, and G. Rowlands, Phys. Rev. A **83**, 013626 (2011).

[29] R. Barnett, A. Turner, and E. Demler, Phys. Rev. Lett. **97**, 180412 (2006).

[30] H. Saito and M. Ueda, Phys. Rev. A **72**, 023610 (2005).

[31] N. P. Robins, W. Zhang, E. A. Ostrovskaya, and Y. S. Kivshar, Phys. Rev. A **64**, 021601 (2001).

[32] L. D. Carr, J. Brand, S. Burger, and A. Sanpera, Phys. Rev. A **63**, 051601 (2001).

[33] T. L. Ho, Phys. Rev. Lett. **81**, 742 (1998).

[34] W. Z. Bao and F. Y. Lim, SIAM J. Sci. Comput. **30**, 1925 (2008).

[35] C. J. Pethick and H. Smith, *Bose-Einstein Condensation in Dilute Gases* (Cambridge University Press, Cambridge, UK, 2002), Chaps. 6 and 7.

[36] A. D. Jackson, G. M. Kavoulakis, and C. J. Pethick, Phys. Rev. A **58**, 2417 (1998).

[37] V. V. Konotop and L. Pitaevskii, Phys. Rev. Lett. **93**, 240403 (2004).

[38] M. S. Chang, Q. S. Qin, W. X. Zhang, L. You, and M. S. Chapman, Nature Phys. **1**, 111 (2005).